Journal of Power Sources 196 (2011) 6366–6373

Contents lists available at ScienceDirect

Journal of Power Sources

journal homepage: www.elsevier.com/locate/jpowsour

Methanol steam reforming in microreactor with constructal tree-shaped network

Yongping Chen*, Chengbin Zhang, Rui Wu, Mingheng Shi

School of Energy and Environment, Southeast University, Nanjing, Jiangsu 210096, PR China

ARTICLE INFO

Article history:
Received 2 February 2011
Received in revised form 16 March 2011
Accepted 23 March 2011
Available online 31 March 2011

Keywords:
Constructal
Methanol steam reforming
Microreactor
Fuel cell

ABSTRACT

The constructal tree-shaped network is introduced into the design of a methanol steam microreactor in the context of optimization of the flow configuration. A three-dimensional model for methanol steam reaction in this designed microreactor is developed and numerically analyzed. The methanol conversion, CO concentration in the product and the total pressure drop of the gases in the microreactor with constructal tree-shaped network are evaluated and compared with those in the serpentine reactor. It is found that the reaction of methanol steam reforming is enhanced in the constructal tree-shaped microreactor, since the tree-shaped reactor configuration, which acts an optimizer for the reactant distribution, provides a reaction space with larger surface-to-volume ratio and the reduction of reactant velocities in the branches. Compared with the serpentine microreactor, the constructal reactor possesses a higher methanol conversion rate accompanied with a higher CO concentration. The conversion rate of the constructal microreactor is more than 10% over that of serpentine reactor. More particularly, the reduction of flow distance makes the constructal microreactor still possess almost the same pressure drop as the corresponding serpentine reactor, despite that the bifurcations induce extra local pressure loss, and the reduction of channel size in branches also causes pressure losses.

1. Introduction

There is an increasing interest in using methanol as the fuel for fuel cells, whether used directly [1,2] or preprocessed by steam reforming [3], partial oxidation [4], or autothermal reforming [5]. For the applications of portable electrical power, of special interest is methanol steam reforming to produce hydrogen for the proton exchange membrane fuel cells (PEMFC), due to its high volumetric energy densities, relatively low operating temperatures, high hydrogen yield and low CO production [3,6,7]. One of the most important challenges for the use of PEMFC with methanol steam reforming in portable applications is the availability of a compact and light unit of fuel reformer with high hydrogen production efficiency. Fortunately, microreaction technology provided a good solution to meet this challenge since it not only can reduce the volume of the chemical devices but also does significantly enhance the reaction process and mass transfer [8]. In particular, a lot of methanol steam microreformers have been designed and investigated to supply hydrogen in the past decades [3,9].

Kawamura et al. [10] designed a microreformer with serpentine microchannel for the supply of hydrogen for a small PEMFC. This micro-reformer demonstrated to be capable of maintaining a hydrogen production rate suitable for powering 1 W-class devices such as cellular phones. Park et al. [11] fabricated a methanol steam microreformer with serpentine microchannel on a silicon wafer by MEMS facilities. The reforming rate, heat transfer and fluid flow through the reformer are experimentally and numerically investigated. Chen et al. [12] designed a plate-type microreformer constructed by parallel microchannels with a diagonal inlet/outlet and numerically analyzed the effects of liquid feed rate, reaction temperature, and steam to methanol ratio on the concentration profiles of methanol, hydrogen, and carbon monoxide in the reactor. Lee et al. [13] compared the reacting flow in a packed-bed reactor and a wall-coated reactor made of borosilicate glass tubes with an inner/outer diameter of 1.5 mm/1.8 mm. They found that the wall-coated reformer has a smaller power requirement for delivering fuel than that of packed catalytic bed reformer. And the thermal resistance of coated-catalytic layer is also smaller. Hsueh et al. [14] numerically investigated a plate steam methanol microreformer with parallel microchnannels. The effects of geometric sizes (aspect ratios and micro channel size) and thermo-fluid parameters (Reynolds number and wall temperature) on methanol conversion and local transport phenomena were explored.

Kundu et al. [15] compared the performance between a parallel channeled and a serpentine channeled microreformer. It was indicated that the performance of the serpentine channeled micro-reformer is always higher than that of parallel channeled micro-reformer. Pattekar and Kothare [16] developed a novel radial flow packed-bed microreactor for hydrogen generation. The microreactor can provide an order of magnitude reduction in the

* Corresponding author. Tel.: +86 25 8379 3092; fax: +86 25 8361 5736.
E-mail address: ypchen@seu.edu.cn (Y. Chen).

0378-7753/$ – see front matter © 2011 Elsevier B.V. All rights reserved.
doi:10.1016/j.jpowsour.2011.03.044

Nomenclature

A, B	Pre-exponential term in the Arrhenius expression
c_i	Mole concentration of species i, mol m^{-3}
c_p	Specific heat, J kg^{-1} K
C_D, C_R	Modification factors of decomposition and reforming reaction
d_k	Branch diameter of the kth level, m
D	Length dimension of channel
E_D, E_R	Activation energy in Arrhenius expression for decomposition and reforming reaction, J mol^{-1}
h	Depth of channels, m
h_j	Enthalpy of species j
ΔH	Enthalpy of reaction, J mol^{-1}
$\vec{J}_i$	Diffusion flux of species i, kg m^{-1} K^{-1}
k_i	Thermal conductivity of species i, W m^{-1} K^{-1}
k_m	Thermal conductivity of the mixture, W m^{-1} K^{-1}
k_D, k_R, k_S	Rate constant for decomposition reaction, reforming reaction and shift reaction
Kn	Knudsen number
l	Characteristic geometric dimension of the channel, m
L_k	Branch length of the kth level, m
L_x, L_y, L_z	Length of the microreactors in the x, y, z direction (m)
M	Molecular weight, kg mol^{-1}
p	Pressure, Pa
r_i	Molar rate of creation/destruction of species i, mol s^{-1} m^{-2}
r_D	Rate of decomposition reaction, mol s^{-1} m^{-2}
r_R	Rate of reforming reaction, mol s^{-1} m^{-2}
Re	Reynolds number
SMR	Steam to methanol molar ratio
T	Temperature, K
$\vec{u}$	Velocity, m s^{-1}
u_{in}	Inlet velocity of reactants, m s^{-1}
w	Width of channels, m
w_{cat}	Catalyst density, kg m^{-2}
x	Conversion of methanol
y_i	Mole fraction of species i
Y_i	Mass fraction of species i

Greek symbols

Δ	Diameter dimension
λ	Molecular mean free path, m
μ	Viscosity, kg m^{-1} s^{-1}

Subscripts

cat	Catalyst
D	Decomposition
i	Species index (1-CH_3OH, 2-H_2O, 3-H_2; 4-CO, 5-CO_2)
in	Inlet
k	Branching level
m	Mixture
out	Outlet
R	Reforming
S	Shift
w	Wall

required driving pressure while maintaining the compact design of the microreactor and providing greater than 98% conversion of methanol to hydrogen at flow rates sufficient to supply fuel to a 20 W fuel cell.

Considering that the flow configuration of a reactor is one of the most important factors to its performance, an appropriate reactor flow configuration will undoubtedly improve the reactant gas transport and the efficiency of thermal management, which results in an improvement in the efficiency of reforming process. However, until now, the most commonly used flow configurations in microreactor still rest on single channel or parallel channels. Therefore, it is desirable to develop a microreactor configuration with optimized conversion and flow performance.

Inspiration for the optimization of many engineering problems can always be found in nature. For example, advanced conversion and flow efficiency can be found in human circulatory and respiratory systems. The flow architectures of the blood-circulating arteries and veins of human beings are self-organized as a branching vessel tree system, and the advanced energy and mass transfer efficiency performs in these architectures. Constructing such branch-tree like architectures is an essential objective of constructal theory which is to describe the geometry and evolution of optimized and organized natural phenomena. The principal of the constructal theory was formulated by Bejan in 1996 as the constructal law of the generation of flow configuration: "For a finite-size flow system to persist in time (to survive) its configuration must evolve in such a way that it provides an easier access to the currents that flow through it" [17,18]. Recent researches have demonstrated that this constructal theory [19,20] has been successfully used to optimize the flow configuration. The important applications of the constructal tree-shaped architectures have been found in electronics cooling [21–24], fuel cells [25–27], traffic [28], etc. Therefore, should we construct similar architectures to optimize the reactor, more advanced transport and reaction performance may be acquired.

In the context, the tree-shaped architecture is introduced to design the methanol steam microreactor in this work. A three-dimensional model for methanol steam reaction in the microreactor with constructal tree-shaped network is developed and numerically analyzed. The methanol conversion, CO concentration in the product and pressure drop of the gases in the microreactor with constructal tree-shaped network are evaluated and compared with those in the microreactor with serpentine flow pattern. In particular, the significant enhancement of chemical reaction in tree-shaped channels is identified and discussed.

2. Construction of a tree-shaped network flow configuration for microreactors

As shown in Fig. 1, a rectangular shape tree-shaped network flow configuration with 6 branching levels can be constructed as [22,23]:

a. Suppose that every channel is divided into two branches at the next level, so $N = 2$, the branching angle φ is 180°, and the tree-shaped network has 6 branching levels as shown in Fig. 1(a).
b. Define that the ratio of the length of the channel at the $(k+1)$th branching level to the length of the channel at the kth branching level as

$$\frac{L_{k+1}}{L_k} = N^{-1/D} \tag{1}$$

It follows that

$$L_k = L_0 N^{-k/D} \tag{2}$$

where L_0 is the length at the 0th branching level. As suggested by Chen and Cheng [22], the energy and mass transfer efficiency at the length dimension $D = 2$ will be the highest, so $D = 2$ is chosen in this work.

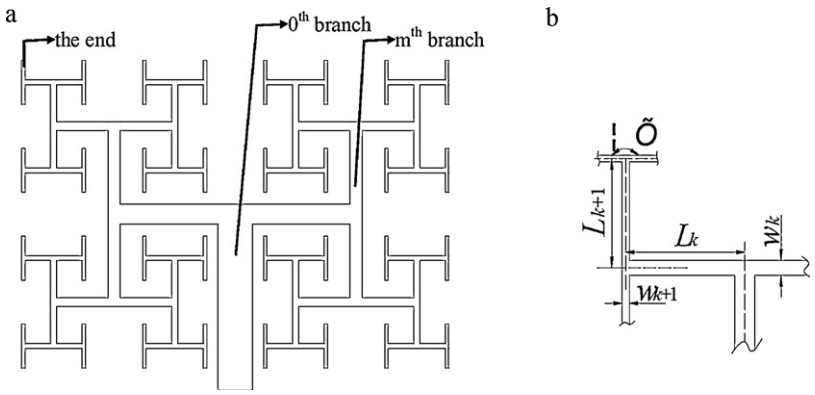

Fig. 1. The schematic of constructal tree-shaped network: (a) tree-shaped network and (b) branches.

c. The branch hydraulic diameters before and after bifurcation are denoted by d_k and d_{k+1}, respectively, and the hydraulic diameter ratio is defined as

$$\frac{d_{k+1}}{d_k} = N^{-1/\Delta} \tag{3}$$

where the diameter dimension $\Delta = 3$ is chosen according to the Murray Law [29]. It follows that

$$d_k = d_0 N^{-k/\Delta} \tag{4}$$

where d_0 is the initial hydraulic diameter of channel network.

In the tree-shaped network configuration, the reduction of channel size leads to a larger reaction surface in a specified volume, which is beneficial to chemical reaction. However, the collection of reactants is difficult to be realized in a single layer tree-shaped net. To solve this problem, the reactor is designed with two layers configuration (i.e. inlet and outlet layers of constructal tree-shaped network), and the inlet layer is of the same distribution of outlet layer except that the 0th branches in the inlet and outlet layers are in the opposite direction. The ends (the highest branching ($k = 6$)) of these two layers are communicated by channels between them as shown in Fig. 2(a) and (b). The cross section of each branch is rectangular and has the same depth of $h = 1$ mm.

To compare the performance of the microreactor with constructal tree-shaped network, a microcreactor with traditional serpentine flow configuration as shown in Fig. 2(c) with both the same channel volume and overall dimensions (L_x, L_y, L_z as shown in Fig. 2) is designed. In addition, the serpentine flow pattern is also of the same cross section with the initial channel in tree network, i.e. the width $w = 2$ mm, the depth $h = 1$ mm and the total length of the serpentine channel is 110 mm. The geometry parameters for the two reactors are shown in Table 1.

Considering the MEMS technology is widely and easily implemented in the fabrication of microreactors, the silicon wafer is used as the substrate of the microreactors in the simulation. A thin layer of commercial catalyst F3-01($CuO/ZnO/Al_2O_3$) with a thickness of 30 μm is assumed to be uniformly deposited on channel walls.

3. Methanol steam reforming in microreactor

3.1. Mathematical model

The mixture of steam and methanol flows in the microreactor with a specified inlet flow rate, and it is reformed over $CuO/ZnO/Al_2O_3$ catalyst via the following overall reactions [30]:

$$CH_3OH + H_2O \xleftrightarrow{k_R} CO_2 + 3H_2. \quad \text{(reforming)} \tag{5}$$

Some portion of the methanol also decomposes directly to CO and H_2 via the reaction:

$$CH_3OH \xrightarrow{k_D} CO + 2H_2. \quad \text{(decomposition)} \tag{6}$$

In addition, the water-gas shift reaction adjusts the composition of the product gas:

$$CO + H_2O \underset{k'_S}{\overset{k_S}{\longleftrightarrow}} CO_2 + H_2. \quad \text{(shift reaction)} \tag{7}$$

It is documented that the reforming reactions can be considered irreversible, and the shift reaction could be neglected without a substantial loss in accuracy [30]. Therefore, the forward reaction of the reforming reaction and decomposition reaction are under consideration in this paper. The chemical reaction rates of the mixture on the catalyst are described as

$$r_R = w_{cat} k_R c_1 \tag{8a}$$

$$r_D = w_{cat} k_D \tag{8b}$$

where w_{cat} is the catalyst density on the channel wall, c_1 represents the molar concentration of methanol near the catalyst surface, k_R and k_D are the rate constants for reforming reaction and decomposition reaction, respectively. The reaction rate constants depend on the properties of the catalyst and reaction condition. The quantities for the catalyst F3-01($CuO/ZnO/Al_2O_3$) can be related to Amphlett's rate constants [30], which are derived form an Arrhenius reaction:

$$k_R = C_R[A_R + B_R \ln(SMR)] \exp\left(-\frac{E_R}{RT}\right) \tag{9a}$$

$$k_D = C_D A_D \exp\left(-\frac{E_D}{RT}\right) \tag{9b}$$

where SMR is the molar ratio of steam to methanol, A_R, B_R and A_D are Amphlett's constants for reforming and decomposing reaction, respectively. C_R and C_D are the empirically correction factors for reforming and decomposing reactions with the catalyst F3-01($CuO/ZnO/Al_2O_3$), which are 5.5 and 3.5, respectively [31]. The molar rate of creation/destruction of species i can be expressed as

$$r_1 = -r_R - r_D \tag{10a}$$

$$r_2 = -r_R \tag{10b}$$

$$r_3 = 3r_R + 2r_D \tag{10c}$$

$$r_4 = r_D \tag{10d}$$

$$r_5 = r_R \tag{10e}$$

where the subscripts indicate: 1-CH_3OH, 2-H_2O, 3-H_2, 4-CO, and 5-CO_2.

Table 1
Geometry parameters for constructal and serpentine microreactors.

Constructal	k	0	1	2	3	4	5	6
	L_k/mm	10.00	7.07	5.00	3.54	2.50	1.77	1.25
	w_k/mm	2	1.12	0.72	0.50	0.36	0.27	0.20
	h/mm				1			
	Total flow length/mm				62.3			
Serpentine	w/mm				2			
	h/mm				1			
	Total channel length/mm				110			
Overall dimensions		L_x = 20 mm, L_y = 27 mm, L_z = 3 mm						

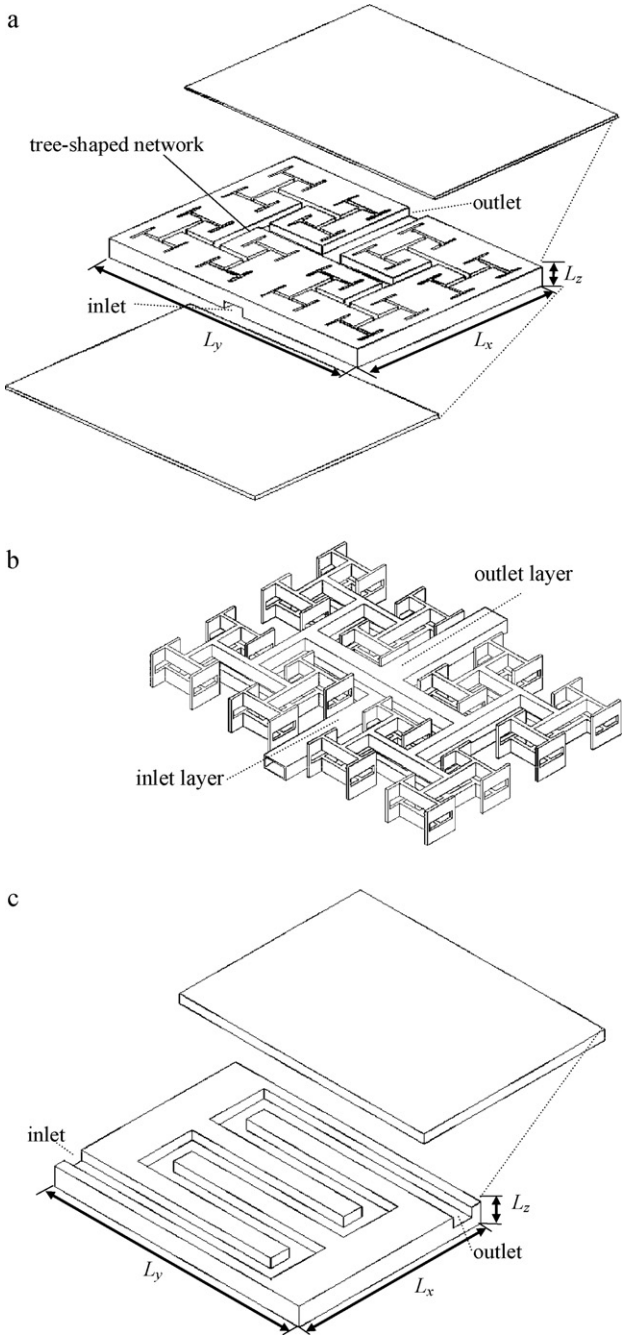

Fig. 2. Schematic of reactors: (a) reactor with constructal tree-shaped network; (b) constructal tree-shaped network; (c) reactor with serpentine flow pattern.

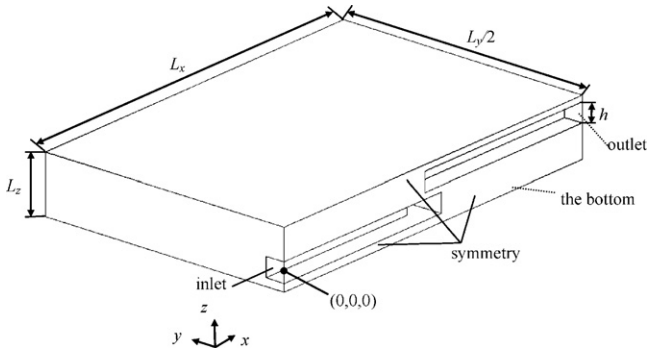

Fig. 3. Computation domain of the microreator with constructal tree-shaped network.

Considering that the microreactor with constructal tree-shaped network is symmetric to the plane of $y = 0$, half of the microreactor, shown in Fig. 3, is selected as the computational domain to simplify the calculation. And the computational domain is the whole microreactor for the serpentine flow pattern reactor. In addition, the following assumptions are applied to the model:

1. Steady state.
2. Negligible gravity.
3. Mixture of the steam and methanol behaves like an ideal gas.

As to the flow in microchannel, the validity of the continuum assumption can be checked by evaluating the Knudsen number (Kn):

$$Kn = \frac{\lambda}{l} \tag{11}$$

where λ is the molecular mean free path and l is the characteristic geometric dimension of the channel. For the smallest channel size, i.e. the 6th hydraulic diameter d_6 = 0.33 mm, the Knudsen number are still far lower than 0.001, which assures the validity of the continuum and Navier–Stokes equations for the systems considered in this work [32]. In addition, the maximum Reynolds numbers under the calculation conditions is no more than 90 in the simulation, so the laminar flow of the mixture is considered.

Thus, the governing equations for the mixture in the microreactors are:

Mass conservation

$$\nabla \cdot (\rho_m \vec{u}) = 0 \tag{12}$$

where the density of the gas mixture, ρ_m, are obtained by ideal gas law.

Momentum conservation

$$\nabla \cdot (\rho_m \vec{u}\vec{u}) = -\nabla p + \nabla \cdot \mu_m \nabla \vec{u} \tag{13}$$

where the viscosity of the gas mixture, μ_m, is computed on the basis of mass fraction average of the pure species

$$\mu_m = \sum_i Y_i \mu_i \tag{14}$$

Species conservation

$$\nabla \cdot (\rho_m \vec{u} Y_i) = -\nabla \cdot \vec{J}_i + M_i r_i \tag{15}$$

where Y_i is the mass fraction of species i, and M_i is the molecular weight of species i. $\vec{J}_i$ is the diffusion flux of species i, which is computed by solving the Maxwell–Stefan equations [33].

Energy conversation

$$\nabla \cdot (\rho_m c_p \vec{u} T) = \nabla \cdot k_m \nabla T - \nabla \cdot (\sum_j h_j \vec{J}_j) - \Delta H_R r_R - \Delta H_D r_D \tag{16}$$

ΔH_R, ΔH_D are the enthalpy of reforming reaction and decomposition reaction respectively and h_j is the enthalpy of species j (j = 1, 2, . . ., 5). The specific heat capacity c_p and thermal conductivity k_m of the gas mixture are obtained from the mass fraction average of the pure species

$$c_p = \sum_1^5 Y_i c_{p,i} \tag{17}$$

$$k_m = \sum_1^5 Y_i k_i \tag{18}$$

For the solid part of the microreactors, there is no mass transport and reaction occurred. The energy conversation

$$\nabla^2 T = 0 \tag{19}$$

Boundary conditions are required to close the mathematical formulation. At the inlet of the microreactor, the velocity, temperature and the steam to methanol molar ratio (SMR) of the methanol steam mixture are specified. The pressure at the outlet is assumed to be atmospheric pressure. Adiabatic boundary conditions are applied to the reactor's external surface except the bottom surface which is assumed as constant wall temperature. Symmetry boundary conditions are applied to the plane at y = 0, which is the symmetric plane of the microreactor. The channel wall is assumed to be no-slip and impermeable, and the continuities boundary of temperature and heat flux is applied as the conjugate boundary condition to couple the energy equations for the fluid and in the wall. It is assumed that there is no catalyst deactivation in the simulation.

3.2. Numerical solution

The set of governing differential equations with the boundary conditions described above for the microreactors is numerically solved with a finite volume scheme, and the pressure-velocity coupling is accomplished by using the SIMPLE algorithm. For the complex constructal structure evaluated, a structured mesh based on hexahedron grid elements is applied to arrive at a solution. The grids near the solid/fluid interface and at bifurcation are specially refined with consideration of the effects of both the boundary layer flow and bifurcation. The resulting system of algebraic equations is solved using the Gauss–Seidal iterative technique, with successive over-relaxation to improve the convergence time. A careful grid-independent study is performed in order to produce grid-independent results. The convergence criteria for the normalized residuals for each variable are restricted to be less than 10^{-6} besides that the normalized residuals for energy is restricted to be less than 10^{-12}. In addition, the solution is regarded as convergent, not only by examining residual levels, but also by monitoring relevant integrated quantities and checking for heat and mass balances.

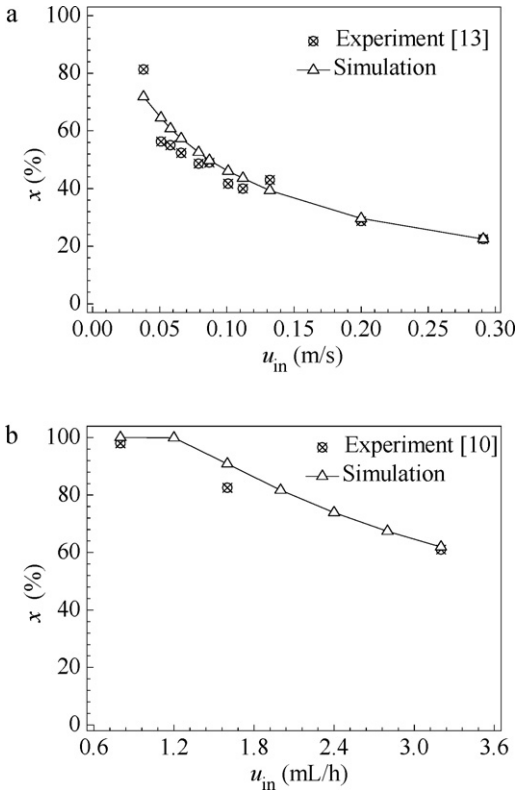

Fig. 4. Comparisons of methanol conversion between numerical results and experimental data: (a) tubular channel and (b) serpentine flow channel.

3.3. Case validation

The experiment of methanol conversion for a wall-coated tubular microreactor with catalyst thickness of 100 μm at 503 K conducted by Lee et al. [13] is numerically estimated using the above model. In addition to the tubular microreactor, the present model is also verified by a miniaturized microreactor with a more complex geometry, serpentine channel [10]. As shown in Fig. 4, the numerical results for these two types of structure are in agreement with the experimental data available in the literature [10,13]. This agreement between the numerical results and the experimental data verifies the present model is reasonable.

4. Numerical results and discussion

In order to evaluate the performance of the reactor for methanol steam reforming reaction, the conversion of methanol and the carbon monoxide (CO) concentration in the product (mixture of H_2, CO_2 and CO at the outlet) are the two main factors. The conversion rate of methanol for the microreactors, x, is calculated by following equation:

$$x = \frac{c_{1,in} - c_{1,out}}{c_{1,in}} \times 100 \tag{20}$$

where $c_{1,in}$ and $c_{1,out}$ are the inlet and outlet molar concentrations of methanol, and the subscript 1 refers to methanol.

Fig. 5 presents the methanol conversion rate and CO concentration as a function of steam to methanol molar ratio (SMR) in the constructal reactor under the conditions of the bottom wall temperatures T_w = 503 K, gas hourly space velocity GHSV = 10,000 h^{-1}, and that the feeding mixtures of steam and methanol is of the same temperature as the bottom wall. As shown in the figures, a larger SMR not only improves methanol conversion rate but also reduces CO concentration in the product. It should be noted that the benefit

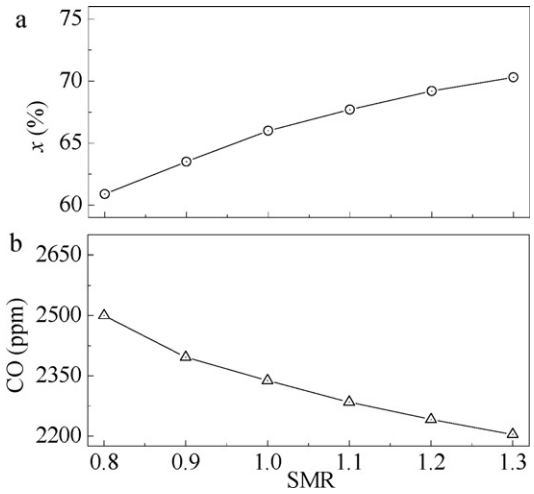

Fig. 5. Effect of molar steam methanol ratios on the performance of constructal reactor (T_w = 503 K and GHSV = 10,000 h^{-1}): (a) methanol conversion rate and (b) CO concentration.

is offset by the increased heating requirement for vaporizing the additional water in the feed. So a compromise value of SMR = 1.1 is utilized in the following simulation.

Fig. 6 plots the variation of the species mole fractions along the flow direction in tree-shaped microreactor. As shown in the figures, the variation range of species mole fractions in the inlet layer is larger than that in the outlet layer. In other words, the reaction rates of the reforming and the decomposition are faster in the inlet layer of tree-shaped network than that in the outlet layer of tree-shaped network, which is induced by larger mole concentration of methanol in upstream. In addition, in the inlet layer of tree-shaped network, the variation of species mole fractions mainly occurs in the region from the 3th branch to the 6th branch. This fact implies that, in the tree-shaped architecture, with the increasing branches, the factors, including the reduction of reactant velocity and larger surface-to-volume ratio owing to the reduction of channel size, lead to enhance the methanol steam reforming process. In order to present a clear understanding of reforming process in tree-shape network, Fig. 7 illustrates the mole fraction of hydrogen at typical cross sections including both in the inlet and outlet layers of tree-

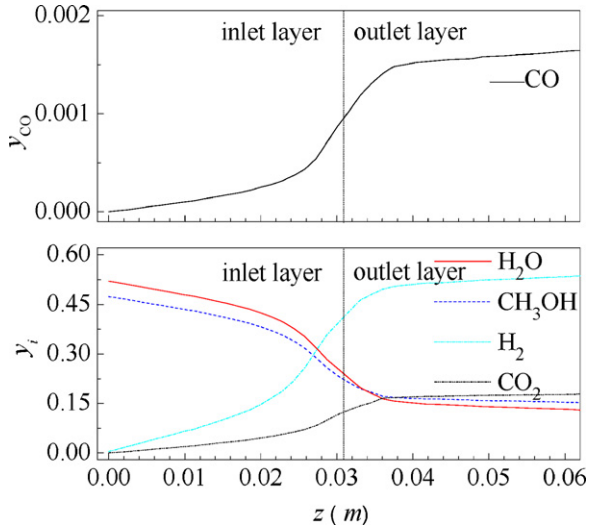

Fig. 6. The variation of mole fractions along the flow direction in constructal microreactor (T_w = 503 K, GHSV = 10,000 h^{-1}, SMR = 1.1).

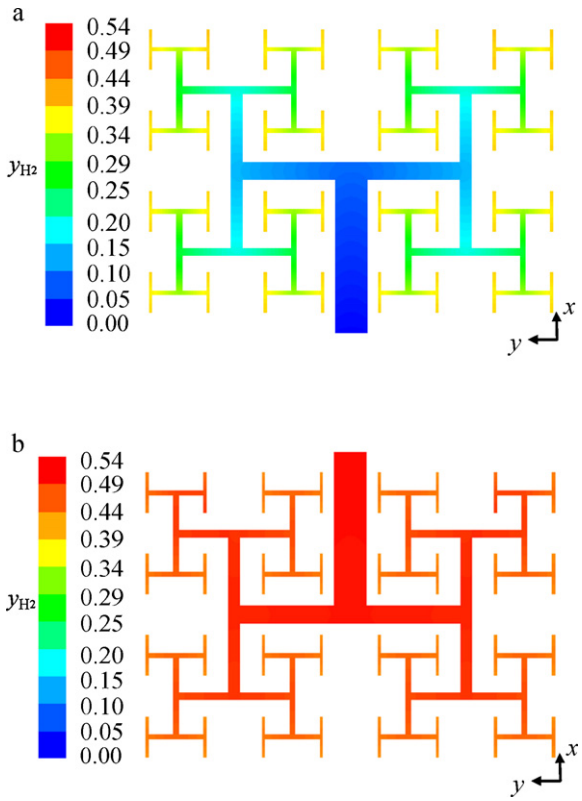

Fig. 7. Distributions of H_2 mole fraction (the same condition as Fig. 6): (a) at z = 0 mm (inlet layer) (b) at z = 1.3 mm (outlet layer).

shaped network. It is indicated by Fig. 7 that the variation of mole fractions of H_2 mainly occurs in the region of latter branch level.

A comparison between the conversion in microreactor with tree-shaped network and microreactor with serpentine flow pattern with respect to the gas hourly space velocities and bottom wall temperatures is presented in Fig. 8. As seen from the figure, the methanol conversion in the constructal microreactor is more than 10% over that of serpentine reactor at the same gas hourly space velocity and bottom wall temperature. The superiority is driven by the fact that, the tree-shaped configuration provides reaction space with larger surface-to-volume ratio owing to the reduction of channel size in the latter branches, and the reactant velocity reduces in the latter branches. It is also indicated by the figure that, both conversion rate in the two types of reactors decrease as the space velocity increases, since the methanol passes through the reactors quickly and has less time to contact with the catalyst with a larger space velocity. And the conversion in these two type reactor obviously increases with the increase of the bottom wall temperature. Therefore, a higher methanol conversion can be obtained under a small space velocity or a higher reaction temperature.

The CO concentrations in both the constructal tree-shaped network microreactor and serpentine microreactor with respect to gas hourly space velocities and the bottom wall temperatures are plotted in Fig. 9. As shown in the figure, both the CO concentrations in the product of the two types of microreators decrease with the increasing space velocity but increase with the increasing reaction temperature, which are of the same trend as the conversion rate. In other words, a higher methanol conversion rate is accompanied with a higher CO concentration in the product. And the CO concentration in the product of the constructal microreactor is a little higher than that of serpentine microreactor.

Fig. 10 compares the total pressure drop between the constructal tree-shaped and serpentine reactors. In the microreactor with

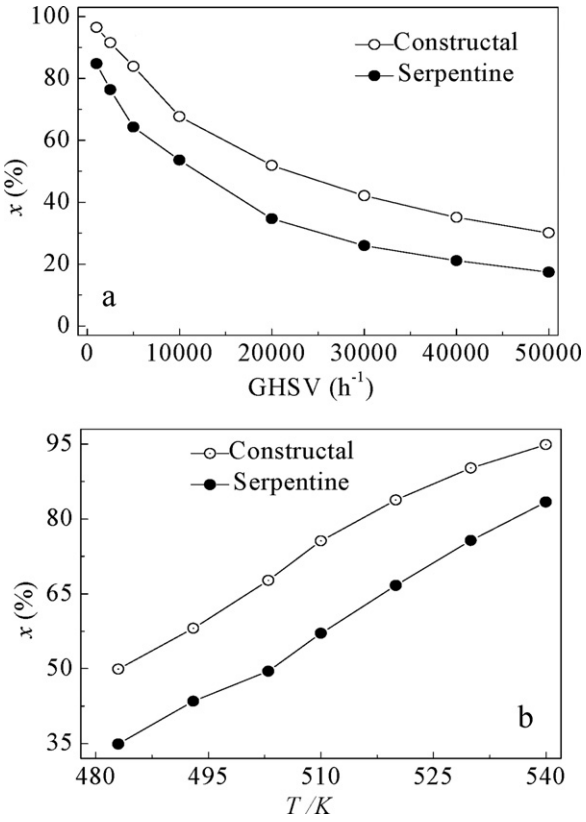

Fig. 8. Comparison of the conversions rate between constructal and serpentine microreactors: (a) T_w = 503 K, (b) GHSV = 10,000 h^{-1}.

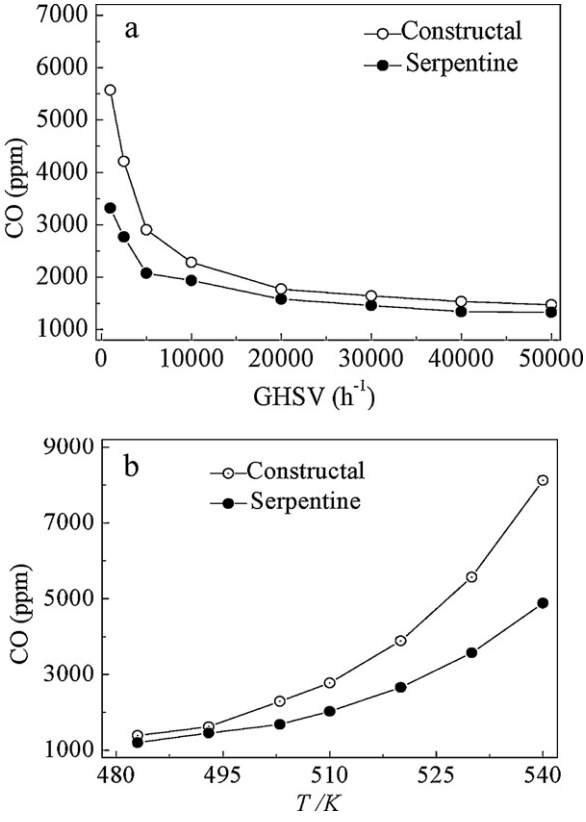

Fig. 9. Comparison of CO concentrations in the product between the constructal and serpertine reactors: (a) T_w = 503 K and (b) GHSV = 10,000 h^{-1}.

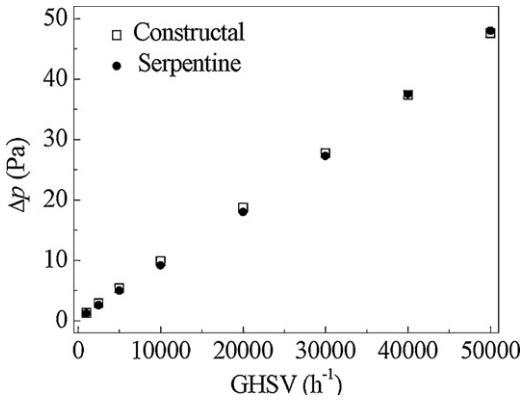

Fig. 10. Pressure drop versus various gas hourly velocities at T_w = 503 K.

tree-shaped network, the local pressure loss is induced by a large number of the bifurcations, and the reduction of channel size in the latter branches also cause pressure losses. However, as shown in Fig. 10, the pressure drop in the microreactor with constructal tree-shaped network is not greater than the microreactor with serpentine flow pattern at various gas hourly space velocities. The primary reason is that the constructal tree-shaped network acts as an optimized fluid transport path which can effectively reduce the flow distance. For the constructal reactor considered in this paper, the flow distance is just 56.6% of the corresponding serpentine reactor. The reduction of flow distance makes the tree-shaped reactor still possess almost the same pressure drop as the serpentine reactor.

5. Conclusion

The constructal tree-shaped network is introduced into the design of the methanol steam microreactors in the context of optimization of flow configuration. A three-dimensional model for methanol steam reaction in this new designed microreactor is developed and numerically analyzed. The methanol conversion, CO concentration in the product and the total pressure drop of the gases in the reactor with constructal tree-shaped network are evaluated and compared with those in a reactor with serpentine flow pattern, which is of the same reaction volume and overall dimensions. The conclusions can be summarized as follows:

(1) Compared with the serpentine reactor, the constructal reactor possesses a higher methanol conversion rate accompanied with a higher CO concentration in the product. The methanol conversion of the constructal microreactor is more than 10% over that of serpentine reactor. This superiority is driven by the fact that, the tree-shaped reactor configuration, which acts an optimizer for the reactant distribution, provides a reaction space with larger surface-to-volume ratio and the reduction of reactant velocities owing to the reduction of channel size in the branches.
(2) In the tree-shaped network, despite the fact that the bifurcations induce extra local pressure loss, and the reduction of channel size in the latter branching level also causes pressure losses, however, the reduction of flow distance makes the reactor with constructal tree-shaped network still possess almost the same pressure drop as the serpentine reactor.

Acknowledgements

The authors gratefully acknowledge the support provided by National Natural Science Foundation of China No. 51076028.

References

[1] S. Wasmus, A. Kuver, J. Electroanal. Chem. 461 (1999) 14–31.
[2] T.S. Zhao, R. Chen, W.W. Yang, C. Xu, J. Power Sources 191 (2009) 185–202.
[3] D.R. Palo, R.A. Dagle, J.D. Holladay, Chem. Rev. 107 (2007) 3992–4021.
[4] L.F. Brown, Int. J. Hydrogen Energy 26 (2001) 381–397.
[5] S. Ahmed, M. Krumpelt, Int. J. Hydrogen Energy 26 (2001) 291–301.
[6] F. Barbir, PEM Fuel Cells: Theory and Practice, Elsevier Academic Press, MA, USA, 2005.
[7] G. Arzamendia, P.M. Diégueza, M. Montesb, M.A. Centenoc, J.A. Odriozolac, L.M. Gandíaa, Catal. Today 143 (2009) 25–31.
[8] W. Ehrfeld, V. Hessel, H. Lowe, Microreactors, Wiley-VCH, Weinheim, 2003.
[9] J.D. Holladay, Y. Wang, E. Jones, Chem. Rev. (104) (2004) 4767–4790.
[10] Y. Kawamura, N. Ogura, T. Yamamoto, A. Igarashi, Chem. Eng. Sci. 61 (2006) 1092–1101.
[11] H.G. Park, J.A. Malen, W.T. Piggott III, J.D. Morse, R. Greif, C.P. Grigoropoulos, J. Microelectromech. Syst. 15 (2006) 976–985.
[12] F.L. Chen, M.H. Chang, C.Y. Kuo, C.Y. Hsueh, W.M. Yan, Energy Fuels 23 (2009) 5092–5098.
[13] M.T. Lee, R. Greif, C.P. Grigoropoulos, H.G. Park, F.K. Hsu, J. Power Sources 166 (2007) 194–201.
[14] C.Y. Hsueh, H.S. Chu, W.M. Yan, J. Power Sources 187 (2009) 535–543.
[15] A. Kundu, J.H. Jang, H.R. Lee, S.H. Kim, J.H. Gil, C.R. Jung, et al., J. Power Sources 162 (2006) 572–578.
[16] A.V. Pattekar, M.V. Kothare, J. Power Sources 147 (2005) 116–127.
[17] A. Bejan, Int. J. Heat Mass Transf. 40 (1997) 799–816.
[18] A. Bejan, M.R. Errera, Fractals 5 (1997) 685–695.
[19] A. Bejan, S. Lorente, Design with Constructal Theory, Wiley, Hoboken, NJ, 2008.
[20] A. Bejan, Shape Structure from Engineering to Nature, Cambridge University Press, Cambridge, 2000.
[21] D.V. Pence, Microscale Thermophys. Eng. 6 (2002) 319–330.
[22] Y.P. Chen, P. Cheng, Int. J. Heat Mass Transf. 45 (2002) 2643–2648.
[23] Y.P. Chen, C.B. Zhang, M.H. Shi, Y.C. Yang, AIChE J. 56 (2010) 2018–2029.
[24] C.B. Zhang, Y.P. Chen, R. Wu, M.H. Shi, Int. J. Heat Mass Transf. 54 (2011) 202–209.
[25] S.M. Senn, D. Poulikakos, J. Appl. Phys. 96 (2004) 842–852.
[26] S.M. Senn, D. Poulikakos, J. Power Sources 130 (2004) 178–191.
[27] S.M. Senn, D. Poulikakos, Int. J. Heat Mass Transf. 49 (2006) 1516–1528.
[28] A. Bejan, J. Adv. Transport. 30 (1996) 85–107.
[29] C.D. Murray, Proc. Natl. Acad. Sci. U.S.A. 12 (1926) 207–214.
[30] J.C. Amphlett, K.A.M. Creber, J.M. Davis, R.F. Mann, B.A. Peppley, D.M. Stokes, Int. J. Hydrogen Energy 19 (1994) 131–137.
[31] S.J. Suh, M.T. Lee, R. Greif, C.P. Grigoropoulos, J. Power Sources 173 (2007) 458–466.
[32] M. Gad-el-Hak, J. Fluid Eng. 121 (1999) 5–33.
[33] H.J. Merk, Appl. Sci. Res. 8 (1958) 73–99.